Materials Science and Engineering B 276 (2022) 115573

Contents lists available at ScienceDirect

Materials Science & Engineering B

journal homepage: www.elsevier.com/locate/mseb

Boosting ion dynamics by developing graphitic carbon Nitride/Carbon hybrid electrode materials for ionogel supercapacitor

Shabeeba Pilathottathil [a,c,*], Jithesh Kavil [b,*], Mohamed Shahin Thayyil [a]

[a] Department of Physics, University of Calicut, Kerala, India
[b] Department of Chemistry, Sree Narayana College, Kannur, Kerala, India
[c] Department of Electronics, Malabar college of advanced studies-Kerala, India

ARTICLE INFO

Keywords:
Supercapacitor
GCN hybrids
Ionogel

ABSTRACT

g-C_3N_3 (GCN) have been used as supercapacitor electrode due to its tunable structure and high carbon–nitrogen ratio, However, the poor conductivity and very low surface area remain a challenge for practical applications. The formation of a hybrid structure of GCN with carbon-based materials such as activated carbon (AC), graphene (G), and carbon nanotube (CNT) help to improve its electrochemical properties. In this work, we synthesized GCN-AC, GCN-G and GCN-CNT hybrid structures and studies the electrochemical properties in symmetric two electrode configuration. The obtained specific capacitance of GCN, GCN-G, GCN-CNT and GCN-AC 11F/g, 244F/g, 237F/g and 266F/g, respectively. The energy density and voltage window of the GCN-AC device were enhanced by replacing the conventional electrolyte with ionic liquid gel electrolyte. The ionogel mediated device could achieve an enhanced specific capacitance of 303F/g with an energy density of 46.45 Wh/Kg and power density of 750 W/Kg.

1. Introduction

The post industrialization have created rapid chaos in our climate due to unprecedented carbon emission which resulted in heat waves, heavy rain falls and irreversible sea level rise. The experts warns the urgent need for the development of an efficient, sustainable and pollution-free energy technology to reduce our carbon foot print [1]. Hence, materials and devices for storage and conversion of energy from renewable energy sources have received significant attention in recent years. The bottle neck in renewable energy technology is the storage of intermittent energy [2]. Lithium ion batteries have been used conventionally as storage device. They use electrochemical mechanism to store energy, that will results in low power delivery and short life of the device. Subsequently, supercapacitor or ultracapacitors appeared as a novel alternative for lithium ion battery. They store charge electrostatically and having high energy density of a battery as well as the high power density of a capacitor [3,4].

To improve their performance, different strategies were cast-off as the use of high capacitive materials with high effective pseudocapacitive materials, better electrolytes having enhanced voltage window keeping in view other practical considerations. Carbonaceous materials such as activated carbon, graphene and carbon nanotubes (CNTs) are commonly used as electrode materials in supercapacitor fabrication, which is known as an electric double-layer capacitor (EDLC) [5]. But still, the systems suffer from low energy density and lower life cycle, which suppresses the practical applications of carbon-based materials. Thus for the realization of supercapacitors, it necessary to design a balanced structure and morphology to increase the electrochemical performance of these carbon-based materials.

The introduction of heteroatoms such as sulfur/nitrogen/phosphorous in the carbonaceous materials can improve electron –donor ability which can further enhance their electrical conductivity by breaking the electroneutrality and density of state [6]. Among these functionalization techniques, the heterostructure with nitrogen doping shows improved results because of its higher electronegativity that effects the net positive charge on the carbon atom in its neighbourhood [7,8]. According to the theoretical prediction, these are the reason for properties enhancements; only one extra electron will be added to the system if carbon is replaced by nitrogen since they are neighbours, the radii of carbon and nitrogen are the same which will help to avoid mismatch of atomic size during functionalization. Further, the nitrogen doping can enhance the electrical conductivity and storage capacity of carbon-based materials [9]. Thus nitrogen functionalization is the key to solve issues regarding carbon-based systems in energy storage applications.

* Corresponding authors.
E-mail addresses: shabeebanawab@malabarcollegevengara.org (S. Pilathottathil), jitheshkavil@gmail.com (J. Kavil).

https://doi.org/10.1016/j.mseb.2021.115573
Received 13 September 2020; Received in revised form 3 November 2021; Accepted 7 December 2021

Recently Graphitic carbon nitride received great dealof attention in supercapacitor device applications due to the polar ring structure, thermal-physical stability, low cost, the abundance of raw material and facile synthesis [10]. Graphitic carbon nitride also can improve the mobility of charge carries, provide more molecule polarity and wettability due to its ring structure with lone pair of electrons in N-atom [11]. GCN exhibits a 2D structure similar to that of grahene however the adjacent carbon atoms in GCN is replaced with N atom. The stacking distance between the aromatic layers of GCN is 0.319 nm, which is lower than that of graphite (0.335 nm) [11]. The improved packing density of GCN provides a stronger binding between the layers and more pleasing charge transport perpendicular to the planes than graphite. However, the practical applications of GCN as electrode material in supercapacitor applications are still in early stages owing to their aggregation, relatively low surface area, the formation of unstable electrode–electrolyte interface and pulverization of electrodes [10]. Hence, the advantages of both GCN and carbon-based material are expected to be integrated into hybrid systems, which will facilitate the electron transport property and energy storage capacity.

Recently carbon coated g-C_3N_4 was prepared by shengang et.al with a specific capacitance (Csp) value 241.6F/g at a current density of 1 A/g. [12] Allam et.al recently developed bio-derived carbon coated g-C_3N_4 inorder to improve the conductity of carbon nitride. They could achieve a Csp value of 300F/g at 1 A/g. [13] Mousavi et. al developed mesoprorous g-C_3N_4/graphene aerogels as supercapacitor electrode. The composite electrode exhibited a Csp of 240F/g at 5 mV/s with excellent cyclic stability. [14] The studies revels that the addition of carbon allotropes could increase the electrical conductivity, surface area and overall electrochemical perfoarmance of g-C_3N_4.

Inspired by the advanced properties of graphitic nitride and carbon-based materials, we developed three hybrid structures of GCN-Activated Carbon (AC), GCN-Graphene(G) and GCN-Carbon Nano Tube (CNT) electrode materials easily and then two-electrode supercapacitor cells were fabricated. The hybrid structures exhibited higher specific capacitance, energy density and power densities than individual materials, which agreed to the theoretical predictions. The electrochemical and physicochemical performance of the hybrid structures proven to be very favorable as energy storage electrodes.

2. Experimental

2.1. Materials

Graphene (500 m^2/g) and CNT (6–13 nm × 2.5–20 μm) were purchased from United Nanotech Innovations, Bangalore, India. Activated carbon was synthesised from charcoal. [5] Polyvinyl alcohol (PVA), n-methyl-2 pyrrolidone (NMP), Charcoal, and sodium sulfate (Na_2SO_4) were purchased from Hi-Media, India. polyvinylidene difluoride (PVDF, 9 wt%, M.W. = 275,000) and Triethyl sulfonium bis (trifluoro methyl-sulfonyl) imide [SEt3][NTf_2]) ionic liquid werepurchased from Sigma Aldrich. GCN and activated carbon were prepared in our lab and if readers need details, refer to our previous publications. [15] PCB with a thickness of 0.048 mm was purchased from audios in Calicut-India. (The information of activated carbon, graphene and CNT is provided in supporting information)

2.2. Synthesis of g-C_3N_4

The graphitic nitride (GCN) was prepared by the high temperature decomposition of thiourea; 10 g of thiourea was dried at 100° C for 24 h and then heated 550 °C/ 4 h in a covered silica crucible. The obtained yellow coloured powder was washed with HNO_3 (0.1 M) followed by deionized water to remove the residual alkaline contents. The powdered sample was then dried at 80 °C/24 h from a hot air oven.

2.3. g-C_3N_4/Graphene, g-C_3N_4/Activated carbon, g-C_3N_4/CNT hybrid samples.

The composite samples of g-C_3N_4 with carbon allotropes such as graphene, activatedcarbon and CNT was prepared by hydrothermal method. The weight ration between g-C_3N_4 and carbon allotropes was fixed to 1: 2 composition. The components were mixed in the specifid ratio by ultrasonication and hydrothermally trated at 100 °C/12 h to get a homogeneous nano-hydrid samples. The precipitates were collected and dried at 80 °C for 5 h from a hot air oven.

2.4. Supercapacitor device fabrication

Printed circuit board (PCB) copper clad is used as a current collector of the supercapacitor devices. The synthesised electroactive materials were mixed with NMP and PVDF in ethanol. The slurry obtained was coated uniformly on the two current collector by a spray coating technique to form symmetric electrodes. The electrodes were dried at 120 °C/6 h from a vaccum oven. Four symmetrical supercapacitors were fabricated by sandwiching GCN, GCN-AC, GCN–G and GCN-CNT electrodes with Na_2SO_4 electrolyte. Please see our previous publications for detailed information about the fabrication process [16].

2.5. Characterization techniques

The surface morphology of prepared samples was studied by field emission scanning electron microscopy (FE-SEM, Carl Zeiss Ultra55). The structural analysis conducted by X-ray diffraction (XRD-Rigaku) by recording patterns from 10° and 90°. The surface area and porosity of prepared samples were analysed by BET analyser (Bruker). Dielectric measurements of electrolytes were carried out using a Novocontrol Alpha dielectric spectrometer (Novocontrol Technologies GmbH, Germany). The experiments were covered in the frequency window of 10^{-2}-10^7 Hz at room temperature. The electrochemical performance of prepared supercapacitors was tested with Sp-logic electrochemical workstation. The cyclic voltammetry (CV), galvanostatic charge–discharge (GCD) cycle and impedance spectroscopy were done to study the capacitive behaviours, stability, storage time and ion diffusion mechanism. The specific capacitance (C_{sp}), gravimetric energy density (E_g) and power density (P_g) were estimated from the slope (dV/dt) of the linear portion of the discharge curve using the following expressions, [17]

$$Csp = \frac{2I\Delta t}{m\Delta V} \quad (1)$$

$$Eg(Wh/Kg) = \frac{1}{8} Csp.V^2 \frac{1000}{3600} \quad (2)$$

$$Pg(W/Kg) = \frac{Eg^*3600}{dischargetime} \quad (3)$$

Where I is the constant current used for charging and discharging, Δt is the discharge time Δv is the potential window and m is the weight of active electrode material in one of the electrodes.

3. Results and discussions

3.1. Crystalline phase analysis

The XRD patterns of as-prepared GCN, GCN-AC, GCN-G, and GCN-CNT are illustrated in Fig. 1, which is used to confirm the crystalline phase of prepared hybrid structures. The peak at 27.1 with an interplanar distance of 0.326 nm (0 0 2) which is the characteristic peak of GCN and it is originated from the layer stacking arrangement of GCN. [18] The diffraction peaks of materials at 13.1 in (0 0 1) plane formed in the crystal due to the presence of in-planar tri-s-triazine units which is imperfect and corresponding to amorphous nature. [19] The amorphous

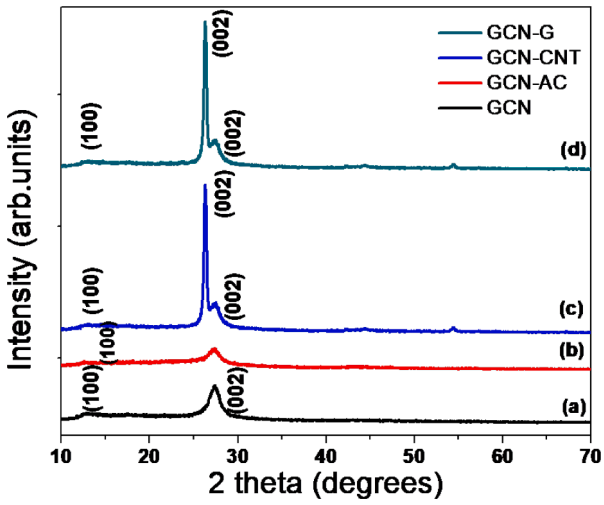

Fig. 1. XRD pattern of GCN, GCN-AC, GCN-G, and GCN-CNT.

nature of materials could enhance the wettability thereby a strong electrode–electrolyte interface is formed and it further increases the charge transport performance which is more pertinent to supercapacitor applications. The peaks at 26.5 in Fig. 1 (a), (b) and (c) is the characteristic peak of carbon allotropes (JCPDS 75–2078). The other peaks at 43.5 and 54.3 in Fig. 1 (c) and (d) is due the reflection from (1 0 0) and (0 0 4) planes of graphene and CNT (JCPDS 00–058–1638).

3.2. Morphology analysis

Fig. 2 shows the SEM images of GCN, GCN-G, GCN-AC, GCN-CNT at 5 μm resolution. The SEM images reveal that the hydrothermal methods allow the formation of hybrid structures without limiting the individual properties of materials. Fig. 2a shows that the GCN is heavily aggregated, which will lead to a decreased surface area. Fig. 2b, c & d show the hybrid structure of GCN-G, GCN-AC, and GCN-CNT, respectively. GCN-AC and GCN-CNT composite samples shows a homogeneous distribution of carbon allotropes in GCN matrix. GCN-AC shows the irregular shaped porous structure with GCN sites and GCN-CNT shows the tubular structure of CNT and some sites are attached with GCN. Hower in GCN-G sample the distribution non-homogeneous with a flake like morphology. The images of hybrid structure proven that materials are combined effectively.

3.3. BET surface area analysis

Fig. 3 represents the Nitrogen adsorption–desorption isotherms spectra of prepared electrode materials. The isotherm of GCN, GCN-G and GCN-CNT shows the type 2 physisorption curve, according to IUPAC which is the characteristic feature of mesoporous materials (pore size in between 2 and 50 nm). [20,21] Type 2 adsorption curves are mainly formed due to the presence of nitrogen and the intermediate flat area of isotherm corresponds to monolayer formation. [22] The surface area of GCN is intrinsically low, however the addition of carbon allotropes, the BET surface area of the electrodes were enhanced considerably. The measured surface area of the electrodes were found to be 26.54, 54. 35, 92. 83 and 823.93 m^2/g respectively for GCN, GCN-G, GCN-CNT and GCN-AC respectively. The GCN-AC electrode exhibits type 1 isotherm curve as shown in Fig. 3d, which depicts the monolayer adsorption. According to Langmuir's theory, type 1 isotherm the distribution of absorbate in between the surface and gas phase. GCN-AC composites show the high surface area, which plays an important role in energy storage applications. The surface area of graphene is intrinsically very large, however GCN-G composite shows very small surface area value due to the non-homogeneous distribution of graphene in GCN matrix.

3.4. Cyclic voltammogram

The electrochemical behaviour of prepared hybrid materials GCN-AC, GCN-G and GCN-CNT as electrode materials for supercapacitors

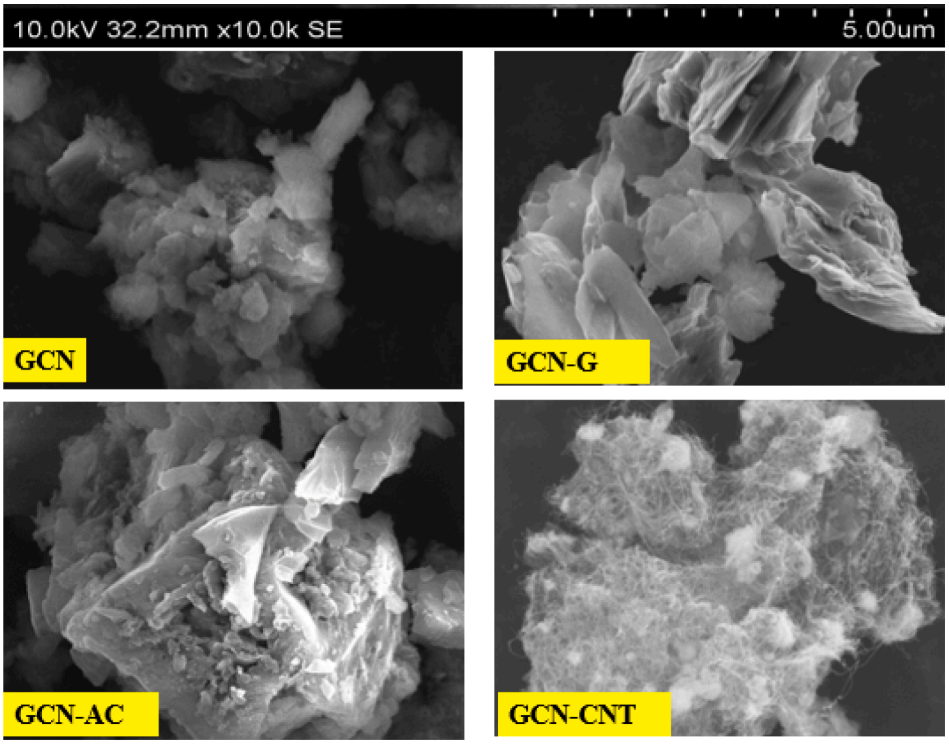

Fig. 2. Surface morphology of prepared electrodes: SEM image of (a) GCN (b) GCN-G (c) GCN-AC (d) GCN-CNT.

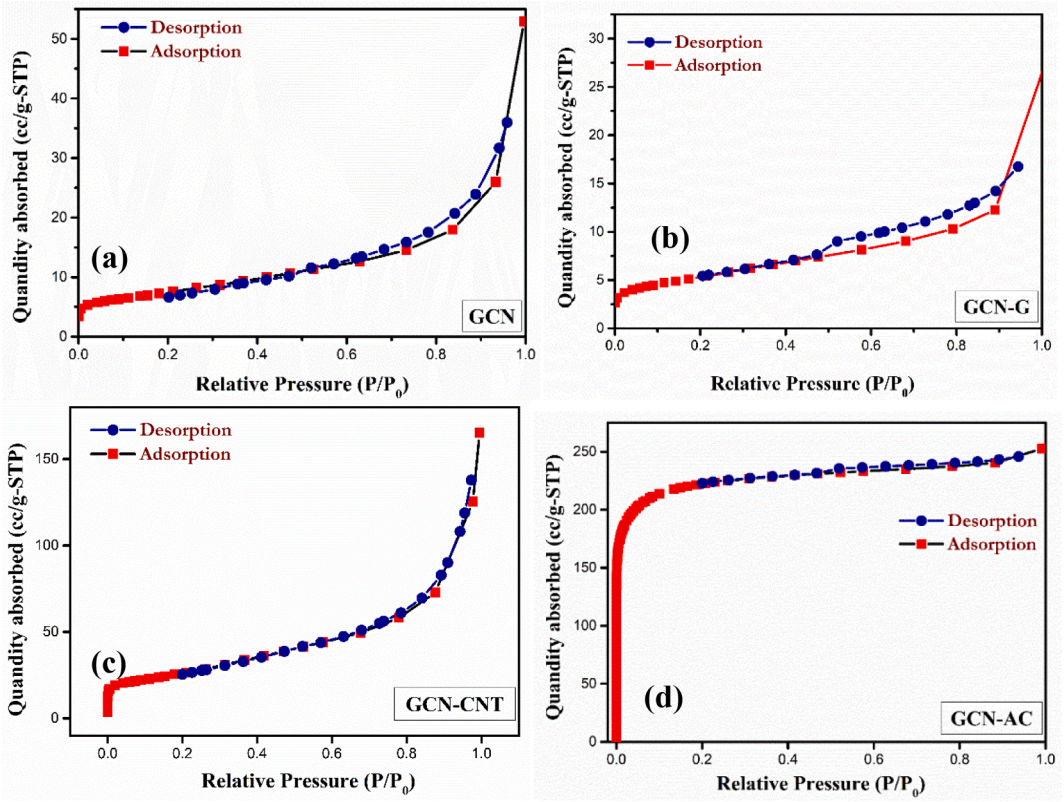

Fig. 3. Adsorption–desorption isotherm for BET analysis of (a) GCN (b) GCN-G (c) GCN-CNT (d) GCN-AC.

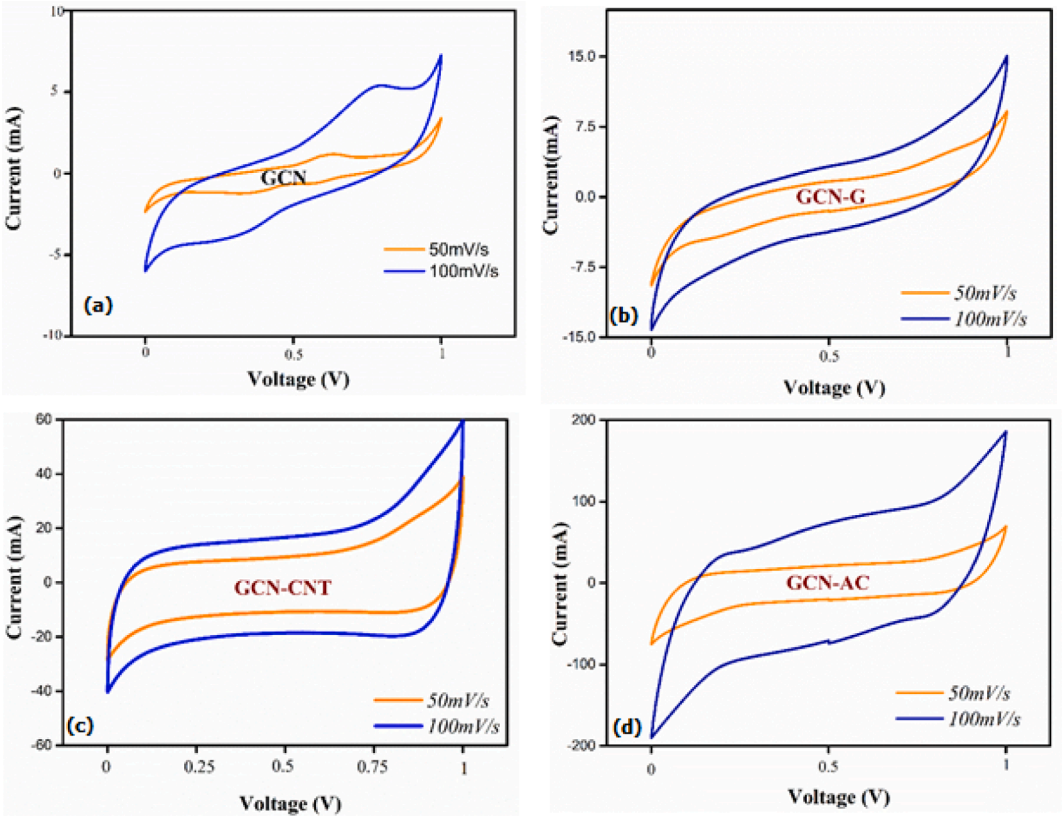

Fig. 4. CV Curves of fabricated supercapacitors with (a) GCN (b) GCN-G (c) GCN-CNT (d) GCN-AC.

were first measured by cyclic voltammetry (CV). The CV curves of GCN and the composites samples at two different scan rates of 50 mV/s and 100 mV/s were given in Fig. 4a, b, c& d respectively. It is clear, the analysis that the hybrid materials show a much larger area for CV curve with almost rectangular type behaviour and higher current response than its bare materials which are the characteristic features of an ideal capacitive material. The calculated specific capacitance of GCN, GCN-G, GCN-CNT and GCN-AC are 11F/g, 244F/g, 237F/g and 266F/g, respectively. The results are in strong agreement with the surface area data. As the surface area increases the specificcapacitance value also increases due to the presence of large number of electro active sites for electrode–electrolyte interactions. [12,15].

3.5. Galvanostatic charge–discharge curve

The actualdevice performance of the synthesied materials as supercapacitor electrodes were analyzed by galvanostatic charge–discharge curves. The GCD were recorded in different current densities of 50 mA and 80 mA as shown in Fig. 5. IR drop of GCN bare electrode supercapacitor is extremely high demonstrating its storage capacity is less and low electrode–electrolyte interactions, it leads to an increase in the internal resistance of supercapacitor devices. On hybridising with carbon allotropes, the pseudo-capacitive behaviour of GCN was masked by the EDLC nature of the additives. Out of the four supercapacitor devices, the duration of the charge–discharge cycle is much high for GCN-AC (Fig. 5 d) with a very small IR drop which is the characteristics of the low overall resistance of the device. As inferred from Fig. 5 the GCN-AC exhibits a high energy density of 8.89 Wh/kg which is extremely higher than the energy density of GCN bare electrode supercapacitors. The energy density and power density of GCN-G and GCN- CNT were also enhanced and the obtained electrochemical results are listed in the Table 2.

Table 1
Electrochemical parameters of fabricated supercapacitors.

Sample Name	Mass (g)	Csp (F/g)	Eg (Wh/Kg)	P (W/Kg)	ESR (Ω)
GCN	0.06	11	0.20	145.83	1.8
GCN-G	0.05	214	7.14	612.50	1.3
GCN-CNT	0.02	237	7.74	175.00	0.9
GCN-AC	0.09	266	8.89	303.13	0.5

3.6. Electrochemical impedance spectra

Further to understand the capacitive behaviour and electronic conductivity of prepared hybrid materials, electrochemical impedance spectroscopy (EIS) test was also conducted over a frequency range of 1 MHz to 1 mHz. Fig. 6 shows the Nyquist plot for GCN, GCN-AC, GCN-CNT and GCN-G electrode supercapacitor in 1 M Na_2SO_4 gel electrolyte. Nyquist plot with a small semicircle and small value at the intersection point on the real axis reveals that the supercapacitor possesses small internal resistance and charge transfer resistance. The nearly vertical line at the low-frequency region directs the ideal capacitive behaviour. [23] The x-intercept on the real axis of all composite is a small value, demonstrating low equivalent series resistance (ESR). The 45° inclination in the mid-frequency region is the characteristics of pore electrode ion diffusion and the semicircle at the frequency region is representing the charge transfer resistance due to faradaic reactions and electric double layer capacitance (EDLC). [24,25] The smaller diameter of semicircle proving the lower impedance, it can be seen that the GCN-AC shows a smaller diameter. From the Nyquist plot, the obtained impedance parameters are listed in Table 1.

3.7. Bode plot

Fig. 6b shows the Bode plot (Phase *Vs.* frequency) curves of prepared hybrid materials, which is seen that the phase angle quickly increases with decreasing frequency at the frequency under 100 Hz and reaching

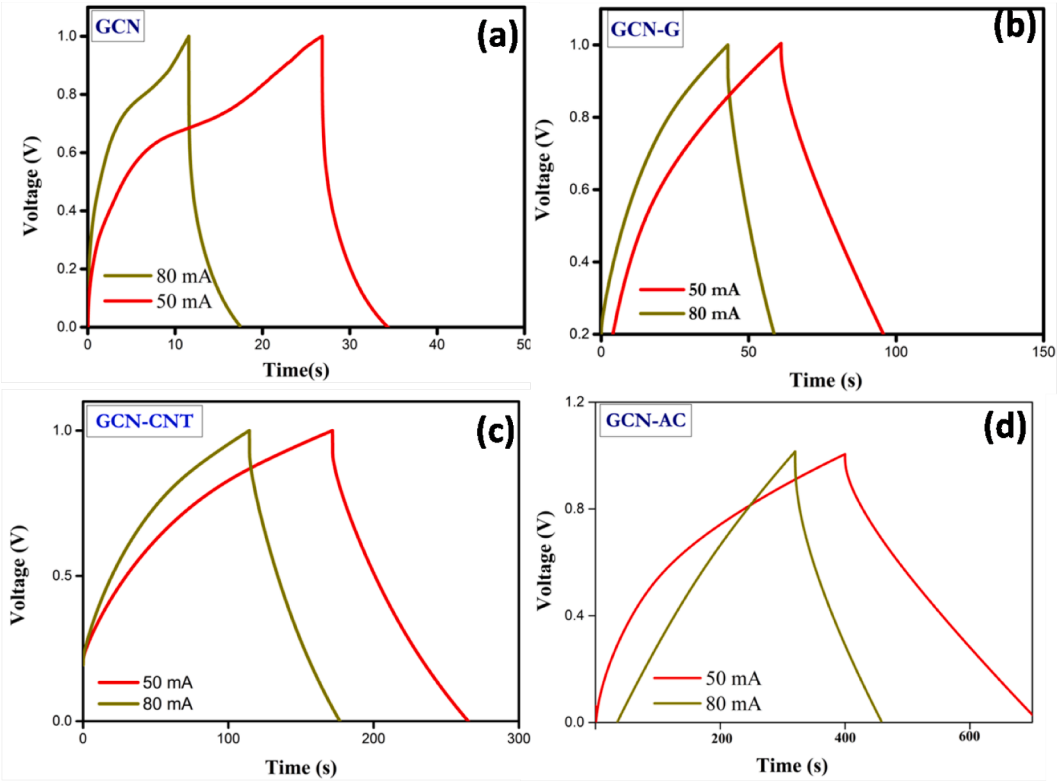

Fig. 5. Galvanostatic Charge Discharge curves: (a) GCN (b) GCN-G (c) GCN-CNT (d) GCN-AC.

Table 2
Comparison of the present research work with similar reports.

Material	Electrolyte/Current density (A/g)	Specific Capacitance (F/g)	Configuration	Reference
Mesoporous carbon nitride (MGCN)/graphene	H_2SO_4, 0.5	240	Three electrode	[14]
g-C_3N_4/functionalized graphene	KOH, 1	265.6	Three electrode	[33]
3D g-C_3N_4/graphene	LiClO4, 0.4	264	Two electrode	[34]
g-C_3N_4/CNT	PVA/H_2SO_4	148	All solid state Two electrode	[35]
g-C_3N_4/graphene	Na_2SO_4, 1	214	Two electrode	Present work
g-C_3N_4/carbon nanotube	Na_2SO_4, 1	237	Two electrode	Present work
g-C_3N_4/activated carbon	Na_2SO_4, 1	266	Two electrode	Present work
g-C_3N_4/activated carbon	Ionic liquid gel electrolyte, 1	303	Two electrode	Present work

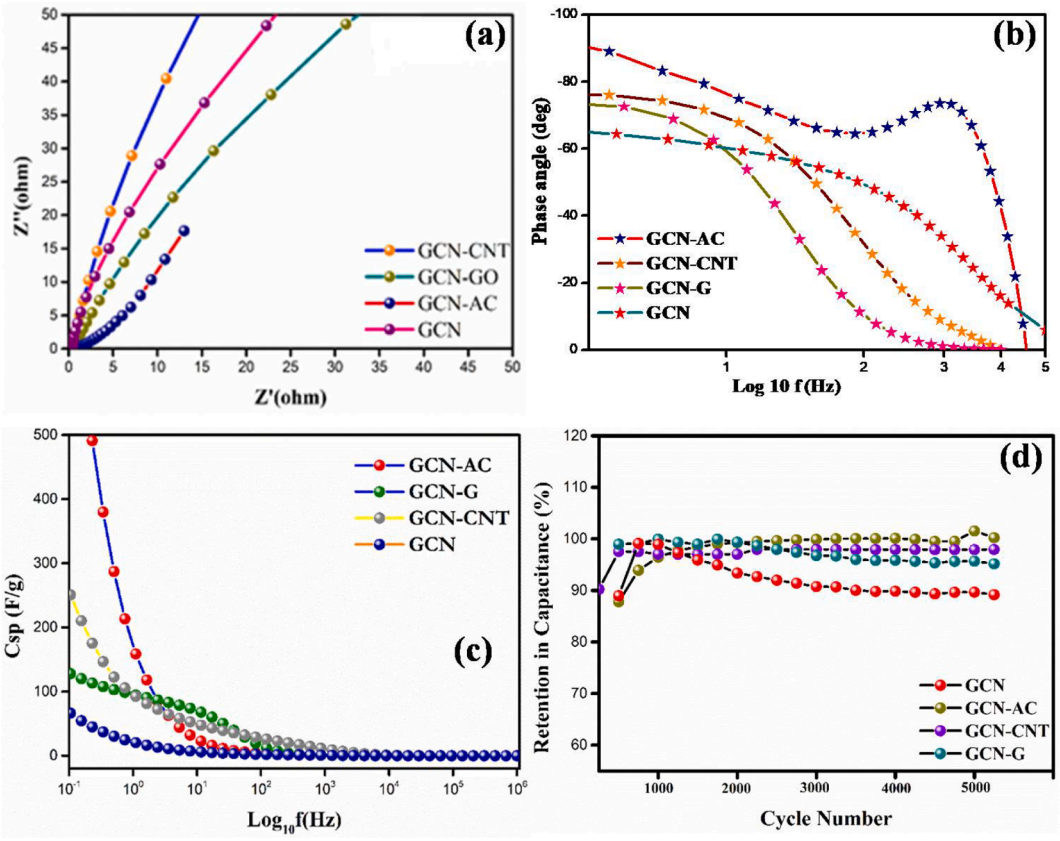

Fig. 6. EIS spectra : (a) Impedance spectra (b) phase angle *vs.* log f (c) Csp*vs.* Log f (d) cyclic stability of fabricated supercapacitors.

to more negative values in the low-frequency region. The hybrid materials are so close to the ideal capacitor value of 90° inclination. Here again, the value of GCN-AC shows the value closer to the ideal value, which means it has excellent capacitive behaviour among others. The obtained specific capacitance *vs* frequency was calculated from the impedance spectral analysis and plotted in the Fig. 6c. Fig. 6 shows GCN-AC composite electrode supercapacitor higher capacitance due to the high surface area of GCN-AC composite, which allows more charge accumulation on the electrode surface. In addition to the good electrochemical performance.

3.8. Cyclic stability

The cyclic stability of hybrid materials and bare GCN supercapacitor devices were recorded over 5000 cycles and according to the results, the hybrid materials enhanced the cyclic stability of the device as shown in Fig. 6d. In general, all these electrochemical results confirm better capacitive performance and rapid charge–discharge property of GCN-carbon based materials composite.

3.9. Ioic liquid/gel electrolyte supercapacitor with wide voltage window

The voltage window of the aforementioned supercapacitor device (GCN-AC) was further improved by fabricating ionic liquid/gel electrolyet based supercapacitor devices. The GCN-AC composites exhibited excellent electrochemical performance in terms of specific capacitance and energy density. However the voltage window of device is limited to 1 V; which is the average voltage of conventional electrolytes. Hence to improve the voltage window, the conventional electrolyte is replaced with electrolytes composed of sulfonyl imide ionic liquid (Triethyl sulfonium bis (trifluoro methylsulfonyl) imide, [SEt3][NTf_2]) mixed with propylene carbonate (PC) organic solvents by keeping the ratio of 25:75. The electrochemical stability window of IL salts in organic solvent resolute at microporous electrodes proposes the possibility of improved voltage window. [26].

3.10. Broadband dielectric spectroscopy (BDS)

To understand the fundamental mechanism of ion dynamics in the

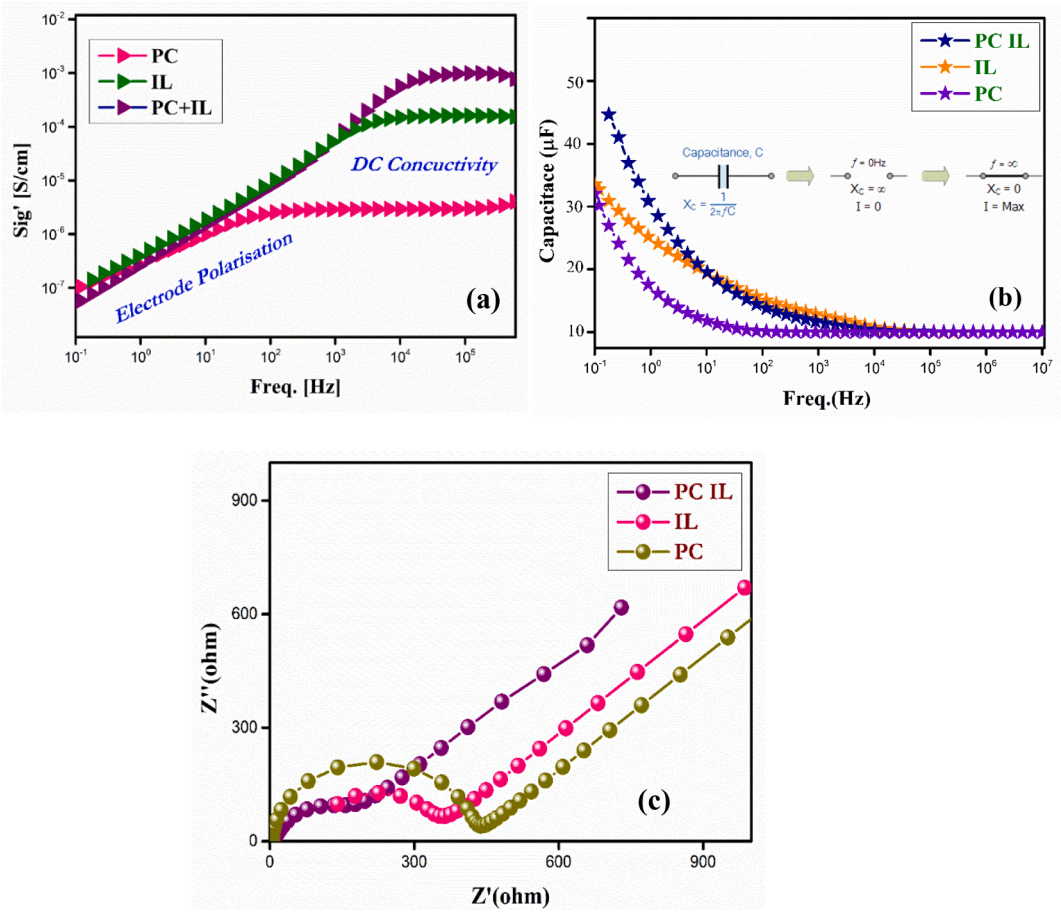

Fig. 7. Broadband dielectric spectroscopic studies of prepared IL electrolyte: (a) conductivity *vs.* frequency (b) capacitance *vs.* frequency (c) cole–cole plot.

proposed electrolyte, the broadband dielectric spectroscopic spectra (BDS) were studied (Fig. 7). There are several factors to estimate the ion diffusivity in the electrolyte system from BDS spectra alone such as electrode polarization, conductivity spectra, frequency dependant capacitance spectra and so on. [27] Fig. 7 (a) shows the conductivity spectra for IL, PC and IL + PC over a frequency range of 10^6 to 10^{-1} Hz at room temperature. All three systems spectra are dominated by the dc conductivity plateau at high-frequency region followed by low amplitude due to electrode polarisations at low-frequency region. From Fig. 7 (a) it can be seen that the mixture of IL + PC enhanced its conductivity to 10^{-3} S/cm. For evaluating capacitive behaviour, the electrolyte is placing in between two electrode, thus a double layer is formed due to the electrode–electrolyte interface. Hence corresponding series capacitance of Helmholtz double-layer and Gouy- Chapman diffuse layer can be described and plotted as in Fig. 7 b. [28] The capacitance value is the representation of the ionic strength of electrolyte. The capacitance *vs.* frequency spectra reveals that the variation of capacitance is high at lower frequency region and constant at the high-frequency region, this is due to the ions have sufficient time to exhibits their real properties at the low-frequency region. [29] Hence the overall performance of the electrolyte can be seen in the low-frequency region. The capacitive behaviour also agrees to the conductivity spectra; the IL + PC shows a high capacitance of 45 μF.

The conduction mechanism of IL + PC further evaluated by impedance spectra over a frequency range of 10^7 to 10^{-1} Hz at room temperature (Fig. 7c). The imaginary and real part of impedance with the same scale of horizontal and vertical axis were plotted as shown in Fig. 7c. From the cole–cole plot for PC, IL and PC + IL, we can see the complex impedance plot consist semicircle and title spike. From the plot, it can be observed that the IL + PC combination showsa small diameter for semicircle, while the PC and IL alone shows a large-diameter semicircle. The small value of diameter indicating low total internal resistance and charge transfer resistance. [30] Additionally, the bulk resistance of the materials is understood from the intercept of semicircle curves and spike lines with the real axis. [31] The conduction of ions in the bulk of electrolyte exhibits semicircle while the tail line is caused due to electrode polarization which is the characteristics of diffusion. The bulk resistance of fabricated supercapacitor with GCN-AC electrode and IL + PC electrolyte calculated from the cole–cole plots is 21 Ω.

3.11. CV, GCD and EIS spaectra of the ionogel supercapacitor device

To further explore the electrochemical practical application potential of GCN-AC electrode with IL + PC electrolyte, asymmetrical supercapacitor was assembled and measured in a two-electrode configuration. As depicted in Fig. 8a the CV curves of fabricated supercapacitor show nearly rectangular shape with increased voltage window and current density, revealing its ideal capacitive behaviour. [32] Moreover, the shape of CV remains unchanged when the scan rates are increased from 50 mV/s to 500 mV/s, indicating outstanding rate performance. Additionally, the GCD measurements at two different current densities are displayed in Fig. 8b. The corresponding specific capacitance of the fabricated supercapacitor with GCN-AC electrode and IL + PC electrolytes at the current density of 1A/g is 303F/g, energy density of 46.45 Wh/Kg and power density of 750 W/Kg. Fig. 8c shows the impedance spectra of fabricated supercapacitor and the intersection of the semicircle at the real axis indicates the equivalent series resistance, the obtained ESR is 25 Ω. These decent electrochemical analyses show that the combination of the GCN-AC electrode with IL + PC is a promising arrangement for high-performance supercapacitor.

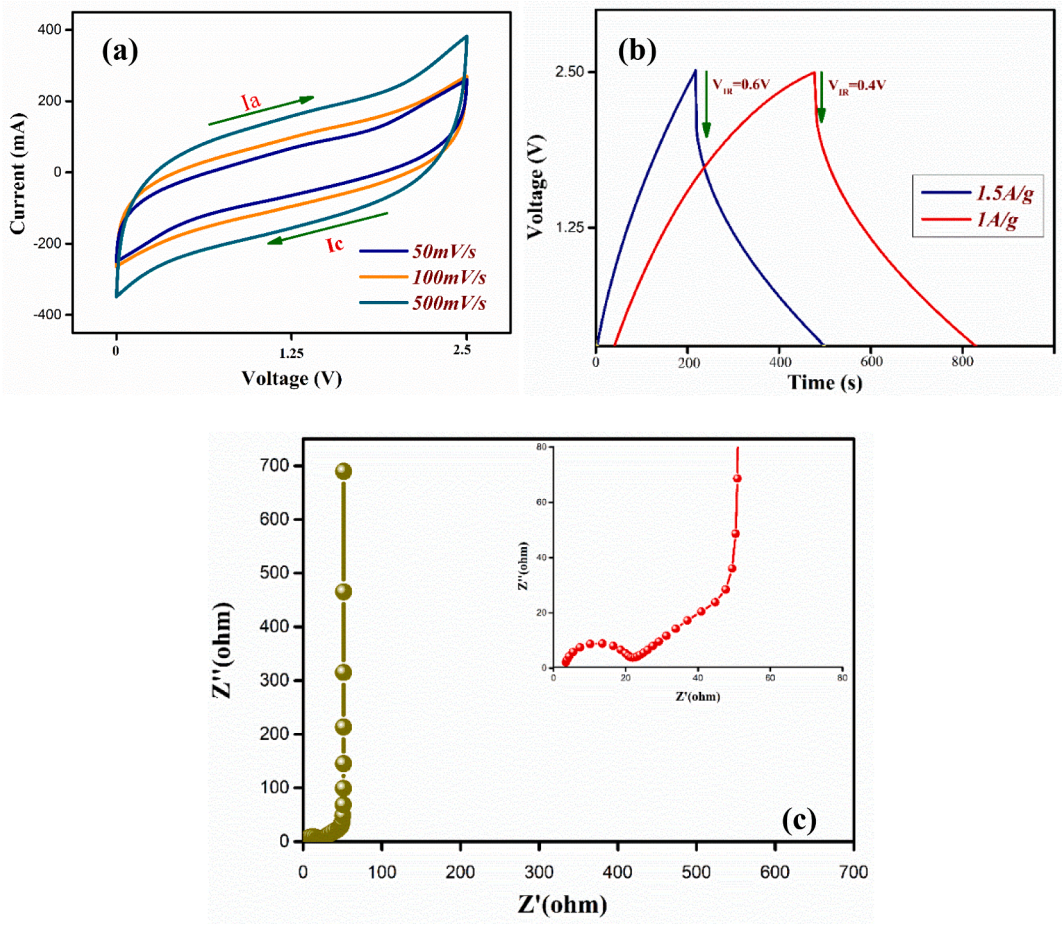

Fig. 8. Electrochemical performance of prepared IL electrolyte: (a) Cyclic voltammetry (b) Galvanostatic charge–discharge cycle (c) Nyquist plot.

Electrochemical properties of g-C_3N_4/carbon allotrope composites were compared with the present work in Table 2.

4. Conclusions

In summary, the g-C_3N_4 based nano-hybrid structures were fabricated from carbon-based materials (AC, Graphene, and CNT). The materials were employed as electrodes in symmetric supercapacitor devices. The composite samples exhibits significant performance improvement in supercapacitor applications when compared to bare GCN electrode. The composites improves the electronic conductivity, enlarges the active sites for surface reaction and wettability. The excellent specific capacitance of 21F/g, 62F/g, 80F/g and 290F/g, were obtained in two electrode system for GCN, GCN-G, GCN-CNT, and GCN-AC electrodes respectively. Moreover, we replaced the conventional electrolyte with ionic liquid (Triethyl sulfonium bis (trifluoro methyl-sulfonyl) imide [SEt3][NTf_2] in propylene carbonate solvent electrolyte for achieving wide voltage window for practical applications. The ionic liquid is a suitable compound for PC based electrolyte system because the pure ILs exhibit high viscosities thus low conductivity at room temperature. Here we tested GCN-AC hybrid material electrode with IL + PC electrolyte based supercapacitor and achieved voltage window of 2.5 V and the specific capacitance of 303F/g. Thus the results proven that the proposed electrode materials are good for both conventional and organic electrolytes.

Declaration of Competing Interest

The authors declare that they have no known competing financial interests or personal relationships that could have appeared to influence the work reported in this paper.

Acknowledgments

Authors thankfully acknowledge fruitful discussions with Pramanic (C-MET Trichur). SP gratefully acknowledges the research fellowship and financial assistance from UGC-JRF. The portion of this research was performed using the facilities at CeNSE, IISc, Bengaluru, funded by Diety, Govt. of Ind and CSIF, University of Calicut.

References

[1] P.A. Owusu, S. Asumadu-sarkodie, A review of renewable energy sources , sustainability issues and climate change mitigation, Civil Environ. Eng. Rev. Article (2016) 1–14, https://doi.org/10.1080/23311916.2016.1167990.
[2] I. Staffell, et al., Environmental Science The role of hydrogen and fuel cells in the global energy system. 463–491 (2019), https://doi.org/10.1039/c8ee01157e.
[3] T.M. Gür, Review of electrical energy storage technologies, materials and systems: challenges and prospects for large-scale grid storage, Energy Environ. Sci. 11 (2018) 2696–2767.
[4] F. Zhang, et al., A high-performance supercapacitor-battery hybrid energy storage device based on graphene-enhanced electrode materials with ultrahigh energy density, Energy Environ. Sci. 6 (2013) 1623–1632.
[5] S. Pilathottathil, K.K. Thasneema, M. Shahin Thayyil, M.P. Pillai, C.V. Niveditha, A high voltage supercapacitor based on ionic liquid with an activated carbon electrode, Mater. Res. Express 4 (2017), 075503.
[6] Y. Cui, et al., Capacitive behavior of chestnut shell-based porous carbon electrode in ionic liquid electrolytes, Colloids Surfaces A Physicochem. Eng. Asp. 508 (2016) 173–177.
[7] A. González, E. Goikolea, J. Andoni, R. Mysyk, Review on supercapacitors : Technologies and materials. 58 (2016) 1189–1206.
[8] J. Safaei, et al., Graphitic carbon nitride (g-C3N4) electrodes for energy conversion and storage: a review on photoelectrochemical water splitting, solar cells and supercapacitors, J. Mater. Chem. A Mater. energy Sustain. 00 (2018) 1–35.

[9] Y. Yang, et al., N-Doped Mesoporous Carbons : From Synthesis to Applications as Metal-Free Reduction Catalysts and Energy Storage Materials. 7 (2019) 1–18.
[10] M.B. Idris, D. Sappani, Unveiling Mesoporous Graphitic Carbon Nitride as a High Performance Electrode Material for Supercapacitors. 11258–11269 (2018), https://doi.org/10.1002/slct.201801752.
[11] J. Safaei, et al., Graphitic carbon nitride (g-C3N4) electrodes for energy conversion and storage: a review on photoelectrochemical water splitting, Solar Cells and Supercapacitors (2018) 22346–22380, https://doi.org/10.1039/c8ta08001a.
[12] Zhi Lin, Ke Wang, Xuezhao Wang, Shijia Wang, Hui Pan, Yingliang Liu, Xu Shengang, Shaokui Cao, Carbon-Coated Graphitic Carbon Nitride Nanotubes for Supercapacitor Applications, ACS Appl. Nano Mater. 3 (7) (2020) 7016–7028.
[13] M.M. Taha, L.G. Ghanem, M.A. Hamza, N.K. Allam, Highly Stable Supercapacitor Devices Based on Three-Dimensional Bioderived Carbon Encapsulated g-C3N4 Nanosheets, ACS Appl. Energy Mater. 4 (9) (2021 Aug 26) 10344–10355.
[14] M. Nazari, M.S. Rahmanifar, A. Noori, W. Li, C. Zhang, M.F. Mousavi, The ordered mesoporous carbon nitride-graphene aerogel nanocomposite for high-performance supercapacitors, J. Power Sources 15 (494) (2021 May), 229741.
[15] P. Shabeeba, M.S. Thayyil, M.P. Pillai, P.P. Soufeena, C.V. Niveditha, Electrochemical Investigation of Activated Carbon Electrode Supercapacitors, Russ. J. Electrochem. 54 (2018).
[16] S. Pilathottathil, M.S. Thayyil, M.P. Pillai, A.P. Jemshihas, Role of a Printed Circuit Board Copper Clad Current Collector in Supercapacitor Application. (2019), https://doi.org/10.1007/s11664-019-07365-6.
[17] Anothumakkool, B., T, A. T. A. & Bhange, S. N. Electrodeposited Polyethylenedioxythiophene with Infiltrated Gel Electrolyte Interface : A Close Contest of an All-Solid-State Supercapacitor with its Liquid-State Counterpart. 1–12 (2014).
[18] D. Prashad, H. Prakash, H. Joo, Decoration of g-C 3 N 4 with hydrothermally synthesized FeWO 4 nanorods as the high-performance supercapacitors, Chem. Phys. Lett. 712 (2018) 83–88.
[19] W.-J. Ong, L.-L. Tan, Y.H. Ng, S.-T. Yong, S.-P. Chai, Graphitic Carbon Nitride (g-C3N4)-Based Photocatalysts for Artificial Photosynthesis and Environmental Remediation: Are We a Step Closer To Achieving Sustainability? Chem. Rev. 116 (2016) 7159–7329.
[20] K.A. Cychosz, M. Thommes, Progress in the Physisorption Characterization of Nanoporous Gas Storage Materials. 4 (2018) 559–566.
[21] Q. Chen, et al., Study on Shale Adsorption Equation Based on Monolayer Adsorption, Multilayer Adsorption, and Capillary Condensation. (2017).
[22] C. Yang, et al., Applied Surface Science High-performance flexible all-solid-state supercapacitors based on densely-packed graphene / polypyrrole nanoparticle papers, Appl. Surf. Sci. 387 (2016) 666–673.
[23] Electrochemical and dielectric studies, Pilathottathil, S., Kannan Kottummal, T., Thayyil, M. S., Mahadevan Perumal, P. & Ambichi Purakakath, J. Inorganic salt grafted ionic liquid gel electrolytes for efficient solid state supercapacitors, J. Mol. Liq. 264 (2018) 72–79.
[24] B. Mei, O. Munteshari, J. Lau, B. Dunn, L. Pilon, Physical Interpretations of Nyquist Plots for EDLC Electrodes and Devices. (2018), https://doi.org/10.1021/acs.jpcc.7b10582.
[25] F. Ghasemi, et al., RSC Advances A high performance supercapacitor based on NiO nanoparticles. 52772–52781 (2017), https://doi.org/10.1039/c7ra09060a.
[26] W. Lu, K. Henry, C. Turchi, J. Pellegrino, Incorporating Ionic Liquid Electrolytes into Polymer Gels for Solid-State Ultracapacitors. (2008), https://doi.org/10.1149/1.2869202.
[27] K. Adrjanowicz, et al., Molecular mobility in liquid and glassy states of Telmisartan (TEL) studied by Broadband Dielectric Spectroscopy, Eur. J. Pharm. Sci. 38 (2009) 395–404.
[28] F. Kremer, A. Schönhals, Broadband Dielectric, Spectroscopy. (2012), https://doi.org/10.1007/978-3-642-56120-7.
[29] T. Cosby, Z. Vicars, E.U. Mapesa, K. Tsunashima, J. Sangoro, Charge transport and dipolar relaxations in phosphonium-based ionic liquids, J. Chem. Phys. 147 (2017) 382–386.
[30] P. Shabeeba, K.K. Thasneema, M.S. Thayyil, M.P. Pillai, C.V. Niveditha, A graphene-based flexible supercapacitor using trihexyl(tetradecyl)phosphonium bis(trifluoromethanesulfonyl)imide ionic liquid electrolyte, Mater. Res. Express 4 (2017), 085501.
[31] Y.J. Kang, Y. Yoo, W. Kim, 3-V Solid-State Flexible Supercapacitors with Ionic-Liquid-Based Polymer Gel Electrolyte for AC Line Filtering, ACS Appl. Mater. Interfaces 8 (2016) 13909–13917.
[32] R. Raman, L.S. Aravinda, R. Rajarao, B. Ramachandra, V. Sahajwalla, Activated carbon derived from non-metallic printed circuit board waste for supercapacitor application, Electrochim. Acta 211 (2016) 488–498.
[33] R. Lin, Z. Li, D.I. Abou El Amaiem, B. Zhang, D.J. Brett, G. He, I.P. Parkin, A general method for boosting the supercapacitor performance of graphitic carbon nitride/graphene hybrids, J. Mater. Chem. A 5 (48) (2017) 25545–25554.
[34] Q. Chen, Y. Zhao, X. Huang, N. Chen, L. Qu, Three-dimensional graphitic carbon nitride functionalized graphene-based high-performance supercapacitors, J. Mater. Chem. A 3 (13) (2015) 6761–6766.
[35] C. Lu, X. Chen, Carbon nanotubes/graphitic carbon nitride nanocomposites for all-solid-state supercapacitors, Sci. China Technol. Sci. 63 (9) (2020 Sep) 1714–1720.